

A Tight Upper Bound on Capacity of Intelligent Reflecting Surface Transmissions Towards 6G Networks

Kyuhyuk Chung

Professor, Department of Software Science, Dankook University, Korea
khchung@dankook.ac.kr

Abstract

To achieve the higher network capacity and mass connectivity in the forthcoming mobile network, revolutionary technologies have been considered. Recently, an upper bound on capacity of intelligent reflecting surface (IRS) transmissions towards the sixth generation (6G) mobile systems has been proposed. In this paper, we consider a tighter upper bound on capacity of IRS transmissions than the existing upper bound. First, using integration by parts, we derive an upper bound on capacity of IRS transmissions under Rician fading channels and a Rayleigh fading channel. Then, we show numerically that the proposed upper bound is closer to Monte Carlo simulations than the existing upper bound. Furthermore, we also demonstrate that the bounding error of the proposed upper bound is much smaller than that of the existing upper bound, and the superiority of the proposed upper bound over the existing upper bound becomes more significant as the signal-to-noise ratio (SNR) increases.

Keywords: *Intelligent reflecting surface, 6G, Rician fading channel, 5G, Upper bound.*

1. Introduction

The paradigm of mobile systems has been shifting from the fifth-generation (5G) communication to the sixth-generation (6G) communication [1]. To this end, international standardization bodies have considered intelligent reflecting surface (IRS) transmissions towards the 6G network [2-4]. Meanwhile, one of 5G technologies is non-orthogonal multiple access (NOMA) [5-7]. The non-SIC NOMA scheme without rate loss was investigated for asymmetric 2PAM [8]. The 3-user low-correlated SC NOMA was proposed with an inflated achievable sum rate [9]. In addition, the 3-user cross CSC NOMA was considered for a higher spectral efficiency in 5G Systems [10]. Also, the performance of weaker channel user in non-uniform source SSC NOMA with novel BTS has been analyzed [11].

In this paper, we present a tighter upper bound on capacity of IRS transmissions compared to the existing upper bound. First, we provide an upper bound on capacity of the IRS transmissions under Rician fading channels and a Rayleigh fading channel. Then, we show numerically that the proposed upper bound is closer to Monte Carlo simulations than the existing upper bound. Furthermore, we also demonstrate that the bounding error of the proposed upper bound is much smaller than that of the existing upper bound, and the superiority

Manuscript Received: May. 24, 2022 / Revised: May. 28, 2022 / Accepted: June. 2, 2022

Corresponding Author: khchung@dankook.ac.kr

Tel: +82-32-8005-3237, Fax: +82-504-203-2043

Professor, Department of Software Science, Dankook University, Korea

of the proposed upper bound over the existing upper bound becomes more significant as the signal-to-noise ratio (SNR) increases.

The remainder of this paper is organized as follows. In Section 2, the system model is described. A tighter upper bound on capacity of IRS transmissions is derived in Section 3. The numerical results are discussed in Section 4. Finally, Section 5 concludes the paper.

The main contributions of the paper are summarized as follows:

- We consider a tighter upper bound on capacity of IRS transmissions than the existing upper bound.
- First, we derive an upper bound on capacity of IRS transmissions under Rician fading channels and a Rayleigh fading channel.
- Then, we show numerically that the proposed upper bound is closer to Monte Carlo simulations than the existing upper bound.
- Furthermore, we also demonstrate that the bounding error of the proposed upper bound is much smaller than that of the existing upper bound, and the superiority of the proposed upper bound over the existing upper bound becomes more significant as the signal-to-noise ratio (SNR) increases

2. System and Channel Model

We assume an IRS transmission system from a single-antenna base station to a single-antenna user. There is a direct link between the base station and the user, which is Rayleigh distributed, denoted by h_d with the second moment $\Sigma_d = \mathbb{E}[|h_d|^2]$. The signal r received by the user is expressed by

$$r = h\sqrt{P}s + n, \quad (1)$$

where the average total transmitted power is P , s is the signal with the average unit power, $h = h_d + \mathbf{h}_{br}^T \Theta \mathbf{h}_{ru}$ and $n \sim CN(0, N_0)$ is additive white Gaussian noise (AWGN). For a given number N of reflecting devices, \mathbf{h}_{br} denotes the $N \times 1$ Rician fading channel from the base station to the IRS and \mathbf{h}_{ru} denotes the $N \times 1$ Rician fading channel from the IRS to the cell-edge user. Thus, the channel gains can be expressed as

$$\mathbf{h}_{br} = \frac{1}{\sqrt{d_{br}^{\alpha_{br}}}} \left(\sqrt{\frac{K_{br}}{K_{br}+1}} \bar{\mathbf{h}}_{br} + \sqrt{\frac{1}{K_{br}+1}} \tilde{\mathbf{h}}_{br} \right), \mathbf{h}_{ru} = \frac{1}{\sqrt{d_{ru}^{\alpha_{ru}}}} \left(\sqrt{\frac{K_{ru}}{K_{ru}+1}} \bar{\mathbf{h}}_{ru} + \sqrt{\frac{1}{K_{ru}+1}} \tilde{\mathbf{h}}_{ru} \right), h_d = \frac{1}{\sqrt{d_d^{\alpha_d}}} \tilde{h}_d, \quad (2)$$

where $d_{br}^{\alpha_{br}}, d_{ru}^{\alpha_{ru}}, d_d^{\alpha_d}$ and $\alpha_{br}, \alpha_{ru}, \alpha_d$ denote the distance and path loss exponent, and K_{br}, K_{ru} denotes the Rician factor. $\bar{\mathbf{h}}_{br}, \bar{\mathbf{h}}_{ru}$ denotes the normalized LoS component, and $\tilde{\mathbf{h}}_{br}, \tilde{\mathbf{h}}_{ru}, \tilde{h}_d$ denotes the normalized non-LOS component. The IRS is represented by the diagonal matrix

$$\Theta = \omega \text{diag}(e^{j\theta_1}, \dots, e^{j\theta_N}), \quad (3)$$

where $\omega \in (0, 1]$ is the fixed amplitude reflection coefficient and $\theta_1, \dots, \theta_N$ are the phase-shift variables that

can be optimized by the IRS. The IRS selects the phase-shifts to obtain the maximum channel gain, as follows:

$$|h|_{\max} = |h_d| + \underbrace{\omega \sum_{n=1}^N |(\mathbf{h}_{br})_n (\mathbf{h}_{ru})_n|}_{\xi} = |h_d| + \xi, \quad (4)$$

where $\xi = \omega \sum_{n=1}^N |(\mathbf{h}_{br})_n (\mathbf{h}_{ru})_n|$.

3. Derivation of Tight Upper Bound on Capacity for IRS Transmissions

We now derive a tight upper bound for the ergodic capacity of the IRS transmission over the Rayleigh fading channel and the Rician fading channels. We start the following conditional ergodic capacity given ξ and $|h_d|$

$$R_{\xi, |h_d|}^{(\text{IRS})} = \log_2 \left(1 + \frac{(|h_d| + \xi)^2 P}{N_0} \right). \quad (5)$$

Then we average $R_{\xi, |h_d|}^{(\text{IRS})}$ over the Rayleigh fading distribution,

$$\begin{aligned} R_{\xi}^{(\text{IRS})} &= \mathbb{E}_{|h_2|} \left[R_{\xi, |h_d|}^{(\text{IRS})} \right] \\ &= \int_0^{\infty} \log_2 \left(1 + \frac{(|h_2| + \xi)^2 P}{N_0} \right) e^{-\frac{(|h_2|)^2}{\Sigma_2}} 2 \frac{(|h_2|)}{\Sigma_2} d|h_2| \\ &= \int_0^{\infty} \log_2 \left(1 + \gamma_{b, \text{norm}} \Sigma_2 \left(g_2 + \frac{\xi}{\sqrt{\Sigma_2}} \right)^2 \right) e^{-\frac{(\sqrt{\Sigma_2} g_2)^2}{\Sigma_2}} 2 \frac{(\sqrt{\Sigma_2} g_2)}{\Sigma_2} (\sqrt{\Sigma_2} dg_2) \\ &= \int_0^{\infty} \log_2 \left(1 + \gamma_b (g_2 + \xi_{\text{norm}})^2 \right) e^{-(g_2)^2} 2 g_2 dg_2 \\ &= \int_0^{\infty} \log_2 \left(1 + \gamma_b x^2 \right) e^{-(x - \xi_{\text{norm}})^2} 2 (x - \xi_{\text{norm}}) dx, \end{aligned} \quad (6)$$

where we define the SNR as $\gamma_{b, \text{norm}} = \frac{P}{N_0}$ with $\gamma_b = \Sigma_2 \gamma_{b, \text{norm}}$, $\xi_{\text{norm}} = \frac{\xi}{\sqrt{\Sigma_2}}$, and we change the variables $\sqrt{\Sigma_2} g_2 = |h_2|$ and $x = |g_2| + \xi_{\text{norm}}$. Now we perform the integration by parts

$$\begin{aligned} R_{\xi}^{(\text{IRS})} &= \left[\left(-e^{-(x - \xi_{\text{norm}})^2} \right) \cdot \log_2 \left(1 + \gamma_b x^2 \right) \right]_{x = \xi_{\text{norm}}}^{\infty} - \int_{\xi_{\text{norm}}}^{\infty} \frac{d}{dx} \log_2 \left(1 + \gamma_b x^2 \right) \cdot \left(-e^{-(x - \xi_{\text{norm}})^2} \right) dx \\ &= \log_2 \left(1 + \gamma_b (\xi_{\text{norm}})^2 \right) - \int_{\xi_{\text{norm}}}^{\infty} \frac{2\gamma_b x}{(1 + \gamma_b x^2)} \cdot \left(-e^{-(x - \xi_{\text{norm}})^2} \right) dx \\ &= \log_2 \left(1 + \gamma_b (\xi_{\text{norm}})^2 \right) - \int_{\xi_{\text{norm}}}^{\infty} \frac{2\gamma_b x}{(1 + \gamma_b x^2)} \cdot \left(-e^{-(x - \xi_{\text{norm}})^2} \right) dx, \end{aligned} \quad (7)$$

Here, based on Jensen’s inequality, we have the upper bound as

$$R^{(IRS)} = \mathbb{E}_\xi [R_\xi^{(IRS)}] \leq R_\xi^{(IRS)} (\mathbb{E}[\xi]), \tag{8}$$

where

$$\mathbb{E}[\xi] = \omega N \sqrt{\frac{\pi}{4d_{br}^{\alpha_{br}} (K_{br} + 1)}} L_{\frac{1}{2}}(-K_{br}) \cdot \sqrt{\frac{\pi}{4d_{ru}^{\alpha_{ru}} (K_{ru} + 1)}} L_{\frac{1}{2}}(-K_{ru}) \tag{9}$$

and $L_{\frac{1}{2}}(\bullet)$ denotes the Laguerre polynomial.

4. Numerical Results and Discussions

In this section, to validate the theoretical analysis, we present numerical results. Parameters are used in the simulations as follows: $d_{br}^{\alpha_{br}} = 150$ m, $d_{ru}^{\alpha_{ru}} = 150$ m and $d_d^{\alpha_d} = 200$ m, $\alpha_{br} = 2.0$, $\alpha_{ru} = 2.0$, $\alpha_d = 3.5$, $N = 10$, and $K_{br} = K_{ru} = 1$. To compare the proposed upper bound on the capacity to the existing upper bound [12], the upper bounds are depicted with respect to Monte Carlo simulations, in Fig. 1. As shown in Fig. 1, the proposed upper bound is closer to Monte Carlo simulations than the existing upper bound, over the entire SNR range $2 \times 10^6 < P/N_0 < 3 \times 10^6$.

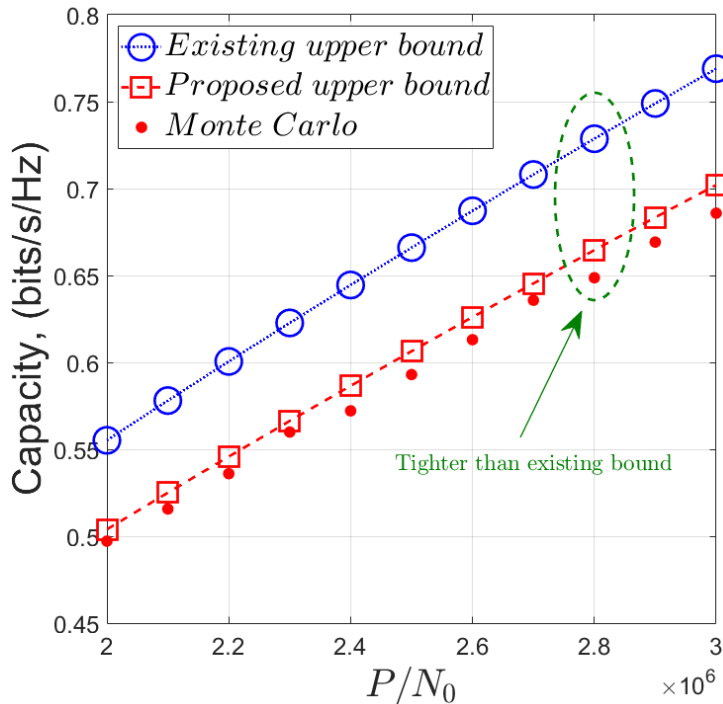


Figure 1. Comparison of proposed upper bound and existing upper bound.

Second, to show the superiority of the proposed upper bound over the existing upper bound, we depict the bounding errors versus the SNR, $0 < P/N_0 < 3 \times 10^6$, in Fig. 2. As shown in Fig. 2, the superiority of the proposed upper bound over the existing upper bound becomes more significant as the SNR increases.

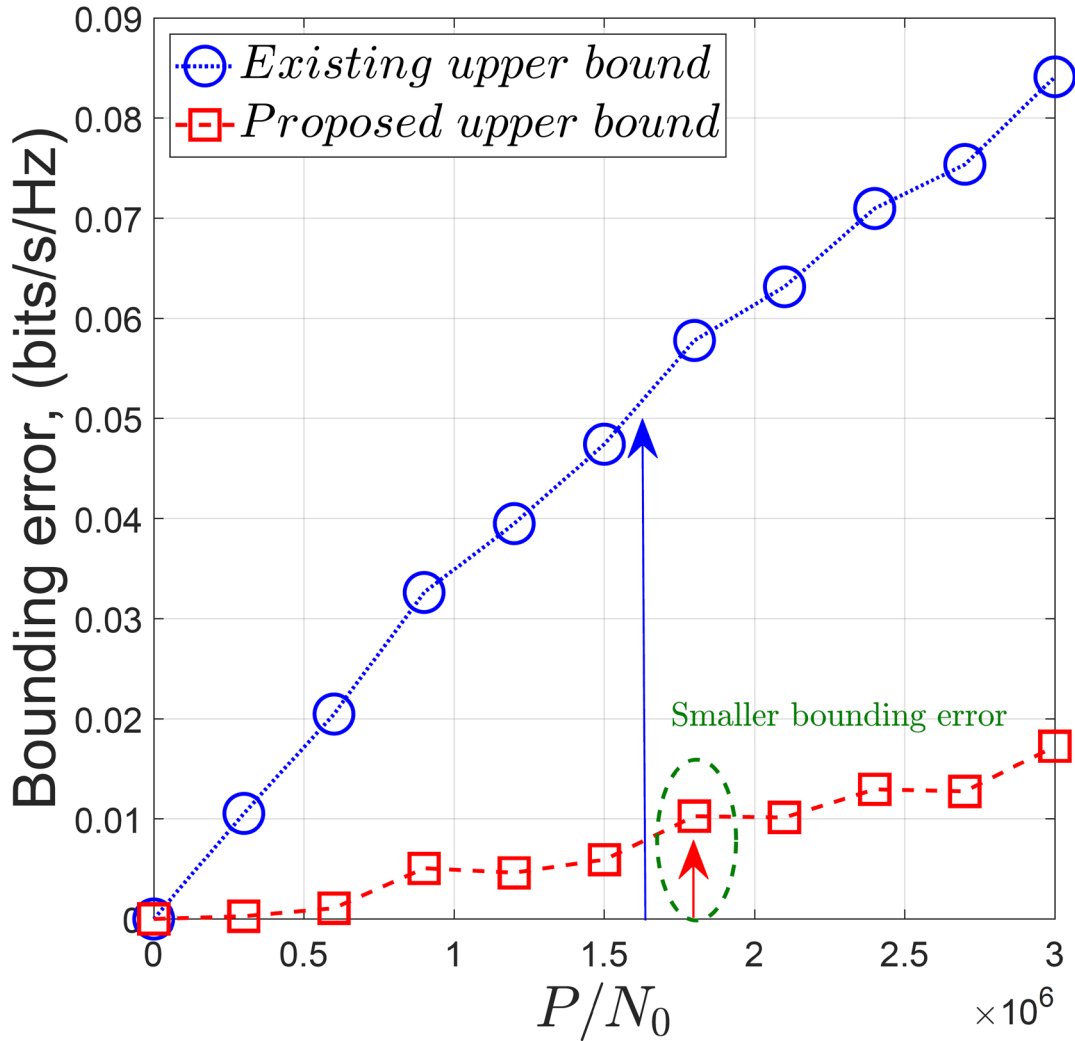


Figure 2. Comparison of bounding error for proposed upper bound and existing upper bound.

5. Conclusion

In the paper, we studied a tighter upper bound on the ergodic capacity of IRS transmissions than the existing upper bound, which has been obtained by applying the Jensen's inequality. Although we also used the Jensen's inequality, we further simplified the expression for the ergodic capacity before applying such inequality. To this end, we specifically used the integration by parts, and the simplified expression reduced the bounding errors. First, using integration by parts, we derived an upper bound on the ergodic capacity of IRS transmissions under Rician fading channels and a Rayleigh fading channel. Then, we showed numerically that the proposed upper bound is closer to Monte Carlo simulations than the existing upper bound. Furthermore, we also demonstrated that the bounding errors of the proposed upper bound are much smaller than those of the

existing upper bound, and the superiority of the proposed upper bound over the existing upper bound becomes more significant as the SNR increases.

References

- [1] E. C. Strinati *et al.*, “6G: The next frontier: From holographic messaging to artificial intelligence using subterahertz and visible light communication,” *IEEE Veh. Technol. Mag.*, vol. 14, no. 3, pp. 42–50, Sept. 2019. DOI: <https://doi.org/10.1109/MVT.2019.2921162>
- [2] Q. Wu and R. Zhang, “Intelligent reflecting surface enhanced wireless network via joint active and passive beamforming,” *IEEE Trans. Wireless Commun.*, vol. 18, no. 11, pp. 5394–5409, Nov. 2019.
- [3] C. Huang, A. Zappone, G. C. Alexandropoulos, M. Debbah, and C. Yuen, “Reconfigurable intelligent surfaces for energy efficiency in wireless communication,” *IEEE Trans. Wireless Commun.*, vol. 18, no. 8, pp. 4157–4170, Aug. 2019.
- [4] Q. Wu and R. Zhang, “Towards smart and reconfigurable environment: Intelligent reflecting surface aided wireless network,” *IEEE Commun. Mag.*, vol. 58, no. 1, pp. 106–112, Jan. 2020.
- [5] Y. Saito, Y. Kishiyama, A. Benjebbour, T. Nakamura, A. Li, and K. Higuchi, “Non-orthogonal multiple access (NOMA) for cellular future radio access,” in *Proc. IEEE 77th Vehicular Technology Conference (VTC Spring)*, pp. 1–5, 2013. DOI: <https://doi.org/10.1109/VTCSpring.2013.6692652>
- [6] Z. Ding, P. Fan, and H. V. Poor, “Impact of user pairing on 5G nonorthogonal multiple-access downlink transmissions,” *IEEE Trans. Veh. Technol.*, vol. 65, no. 8, pp. 6010–6023, Aug. 2016. DOI: <https://doi.org/10.1109/TVT.2015.2480766>
- [7] Z. Ding, X. Lei, G. K. Karagiannidis, R. Schober, J. Yuan, and V. Bhargava, “A survey on non-orthogonal multiple access for 5G networks: Research challenges and future trends,” *IEEE J. Sel. Areas Commun.*, vol. 35, no. 10, pp. 2181–2195, Oct. 2017. DOI: <https://doi.org/10.1109/JSAC.2017.2725519>
- [8] K. Chung, “Achievable power allocation interval of rate-lossless non-SIC NOMA for asymmetric 2PAM,” *International Journal of Advanced Smart Convergence (IJASC)*, vol. 10, no. 2, pp. 1-9, June. 2021. DOI: <http://dx.doi.org/10.7236/IJASC.2021.10.2.1>
- [9] K. Chung, “On Inflated Achievable Sum Rate of 3-User Low-Correlated SC NOMA,” *International Journal of Advanced Smart Convergence (IJASC)*, vol. 10, no. 3, pp. 1-9, Sept. 2021. DOI: <http://dx.doi.org/10.7236/IJASC.2021.10.3.1>
- [10] K. Chung, “Higher Spectral Efficiency of 3-User Cross CSC NOMA in 5G Systems,” *International Journal of Advanced Smart Convergence (IJASC)*, vol. 10, no. 3, pp. 17-25, Sept. 2021. DOI: <http://dx.doi.org/10.7236/IJASC.2021.10.3.17>
- [11] K. Chung, “Performance Analysis for Weaker Channel User in Non-Uniform Source SSC NOMA with Novel BTS,” *International Journal of Advanced Smart Convergence (IJASC)*, vol. 11, no. 1, pp. 36-41, Mar. 2022. DOI: <http://dx.doi.org/10.7236/IJASC.2022.11.1.36>
- [12] Q. Tao, J. Wang, and C. Zhong, “Performance analysis of intelligent reflecting surface aided communication systems,” *IEEE Commun. Lett.*, vol. 24, no. 11, pp. 2464–2468, Nov. 2020. DOI: [10.1109/LCOMM.2020.3011843](https://doi.org/10.1109/LCOMM.2020.3011843)